A Non-Radiating Composite Right-/Left-Handed Transmission Line Derived from Substrate Integrated Rectangular Hollow Waveguide

***Yvonne Weitsch*, Thomas F. Eibert**

Institute of Radio Frequency Technology, Universität Stuttgart, Pfaffenwaldring 47, 70569 Stuttgart, Germany
Phone 0049 711 / 685 – 67411, Fax 0049 711 / 685 – 67412, mail@ihf.uni-stuttgart.de

Abstract

The majority of up-to-date conceived composite right-handed / left-handed (CRHLH) transmission lines (TL) are open configurations derived from microstrip technology. We present here a closed CRHLH architecture derived from the H_{10} rectangular hollow waveguide mode, which is realised in substrate-integrated waveguide (SIW) technology and is thus easy to fabricate. The dispersion characteristic is validated by two separate methods, based on FEM and Matrix-Pencils. The attenuation performance is also examined and proves to be well comparable with peer designs. Prototypes are realised and measured.

1. Introduction

With the disclosure of the concept of composite right-handed / left-handed (CRHLH) transmission lines (TL) [1][2], many structures have been conceived enhancing the electromagnetic performance of engineered devices or even leading to unprecedented functionalities. However, most of the developed meta-compositions are open and thus possibly radiating structures as they are often derived from microstrip technology. In terms of leaky-wave antennas, this power leakage is an essential working mechanism. In contrast, in guided-wave applications the aim is to transmit energy preferably without loosing any energy be it by radiation or by losses. Hollow waveguides offer here attractive solutions as they transport energy with little losses. Conventional hollow waveguides are not constituted on a loss-providing dielectric substrate and the surface currents can spread over a large cross-sectional surface, thus leading to a low resistance. The closed structure proposed in this paper is derived from the rectangular hollow waveguide. The physical nature of its dominant H_{10} mode can be represented by an equivalent electric circuit (EQC), which is well-approved and is reasoned in [3]. It resembles the one of a CRHLH transmission line (Fig. 1). By slight modifications, the missing series capacitance can be introduced. A crucial point is that the proposed architecture operates in its fundamental mode thus ensuring stable and predictable operation. Another potential design of a closed CRHLH TL is a corrugated waveguide such as considered in [4]. However, such a conventional hollow waveguide design is expensive to fabricate and due to the deep corrugations by no means a compact solution. Also, the design presented in [5] does not appear to provide for a simple fabrication procedure. This closed CRHLH TL is derived from a stripline configuration and it is closed at the sides in a box-like manner in order to suppress possible radiation. As hollow waveguide modes in the box-like structure must be avoided, the sidewalls must be placed as close as possible to the inner conductor leading overall to a structure of complicated shape. With the goal to circumvent the elaborate fabrication of a hollow waveguide and being economical, we establish a substrate integrated waveguide (SIW) [6], in which the vertical sidewalls are replaced by rows of vias leading to light weight. It features periodic unit cells which can easily be manufactured by multi-layer printed circuit technology. As we arrive at a sufficient serial capacitance, the unit segments can be kept remarkably short in comparison to wavelength complying the homogeneity criteria of metamaterials and resulting in a compact size. Another issue in metamaterials, especially those based on the theory of CRHLH TLs, is to achieve the balanced state [1]. It means that the series resonant circuit is adjusted to the shunt one, such that their resonant frequencies are identical. For the presented design, the balancing process is easy to handle entailing broadband matching. The final CRHLH waveguide exhibits broad-band matching and low attenuation despite of the constituting dielectric substrate, which is not particularly low-loss. In the following items, we discuss the design aspects of this wideband balanced waveguide in detail. Subsequently, the matching steps are elucidated. The dispersion behaviour is visualised by the dispersion diagram. The eigenmode calculation is validated by two methods, by means of a finite-element (FEM) solver (Ansoft HFSS) and the Matrix-Pencil estimation technique. Simulated as well as measured results are presented.

2. Waveguide Design

Conversely to other lumped or distributed elements CRHLH realizations [1][4][6], the EQC of the H_{10} rectangular waveguide mode [3] provides the fundament for the design proposed in this paper. The missing series

capacitors as compared to the EQC of a CRHLH TL are implemented in a special manner [7][8] reaching an enhanced capacitance and as such especially short periodic sections become possible. However, in [7][8] the configuration is open. Since we wish to design a closed structure which does not loose energy to its environment, we cannot directly work with such a construction. By mirroring the open configuration at the plane with the slots, we obtain the desired closed waveguide. Since such a configuration would be very difficult to fabricate, a simplified design as compared to the fully mirrored set-up is used, where the series capacitors are implemented employing a single Kapton foil layer. The Kapton foil separates two metallic layers of which the lower metallic plate bridges the slots in the upper one so that parts of their faces overlap. Fig. 2 and Fig. 4 picture the inner configuration of the waveguide. The upper level metallic strips on the Kapton foil are short-circuited by via holes with both, the top copper plate and the bottom ground plane of the waveguide. These side arrays of vias limit the SIW in its transverse geometry, prescribing the cut-off frequency of a traditional RH waveguide. The subject here is a CRHLH waveguide, where the cut-off frequency is relieved and wave propagation is enabled below cut-off leading to the LH characteristic. For the CRHLH waveguide, the transverse dimension Δw fixes the value of the shunt resonance. The resonance frequency of the series circuit is controlled by the longitudinal proportions and the series capacitance, which remain to be tuned in order to balance the frequencies. For this reason, establishing the balanced state is very convenient because the decisive design parameters are decoupled from each other. So, the process of balancing is to adjust the length Δl of one unit cell and with it the width of the metallic strips as well as the shared area with the metallic tongue slightly below. The effect becomes visible in the course of the transmission coefficient or similarly in the reflection coefficient, because an unbalanced CRHLH TL provides a band stop. As issued in [1], the characteristic impedance of the transmission line ideally becomes independent from frequency, given the configuration is balanced. For our particular configuration with a transverse distance between the vias of 17.9 mm and $\varepsilon_r = 3.58$, broad-band matching was achieved in a simulation model with a unit cell length Δl of 3.62 mm. 40 unit cells lead to a total length of 184.62 mm of the waveguide. The reflection coefficient encircles the matching point seen in Fig. 3. The good matching performance is not only gained by the appropriate dimensions of the periodic waveguide. An adequately-designed tapered feeding segment supplies the transition to a 50 Ω microstrip line (Fig. 4). Fig. 6 points out that S_{11} in the simulation is less than -14.56 dB for 2.35 GHz up to 5.4 GHz.

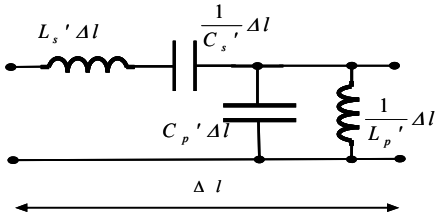

Fig. 1. Equivalent circuit model of a short section Δl of a CRHLH TL

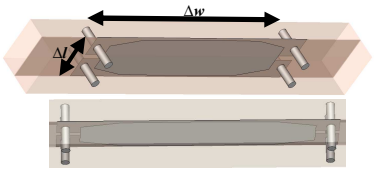

Fig. 2. Unit cell of the periodically assembled waveguide pointing out the circuit model equivalences

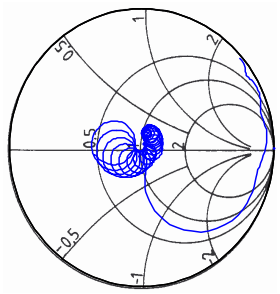

Fig. 3. S_{11} of unit cell with $\Delta l = 3.62$ mm

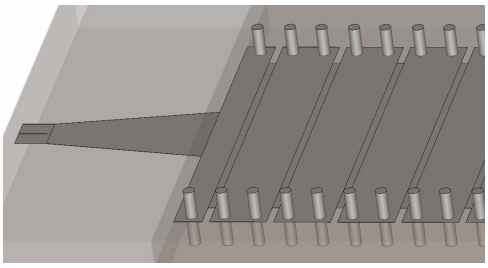

Fig. 4. Detail of the inner waveguide structure including the feeding section. The top and the bottom plates are hidden in the drawing in order to unveil the interior of the structure.

3. Realised Prototype

Two configurations have been manufactured featuring a unit cell length of $\Delta l = 3.95$ mm for prototype 1 and 3.65 mm for model 2. Fig. 5 shows one of the prototypes. In the CST MWS model, the permittivity of the Arlon substrate is defined as $\varepsilon_r = 3.58$ with a $\tan\delta = 0.0035$, the material parameters of the Kapton foil read $\varepsilon_r = 2.8$ with $\tan\delta = 0.003$. Fig. 6 visualises the reflection coefficient of the simulated and balanced model for the frequency range from 2 GHz up to 7 GHz. In Fig. 7, the reflection coefficients of the fabricated structures are given. With the

dimensions of Conf1 $\Delta l = 3.95$ mm, the shunt and the series resonance are not balanced and it does not approach the reflection values of the matched simulation model. Conf2 with $\Delta l = 3.65$ mm mainly achieves reflections to be mostly less than -10 dB and can be considered to nearly reach the balanced situation.

Fig. 5. Realised prototype

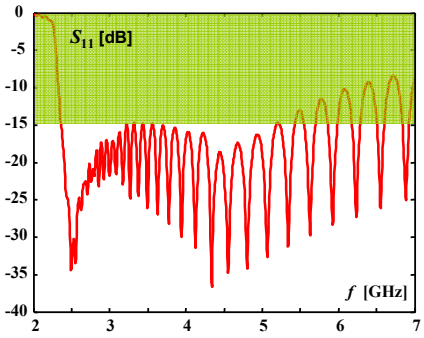

Fig.6. Simulated reflection coefficient

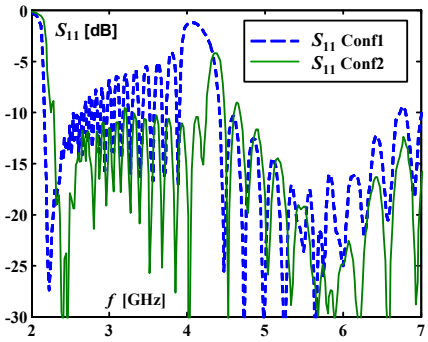

Fig.7. S_{11} of fabricated models

4. Dispersion Diagram

Once a new metamaterial has been created, the proper eigenmodes which uniquely define the material behaviour should be determined. In general, an eigenmode wave function satisfying the Helmholtz equation is expressed in the form

$$\psi = \psi_0 e^{-\gamma z}, \tag{1}$$

if restricted to one-dimensional wave propagation in positive z-direction. Further, the propagation constant γ may be complex composed of the real part α, the attenuation constant, and the imaginary quantity β, also referred to as phase constant or wavenumber. The mathematical nature γ as solution of the eigenvalue equation defines the physical characteristic of the mode. In case it possesses the imaginary value β, the wave propagates. The mathematical interpretation is assisted by a graphical representation in a dispersion diagram, in which normally the eigenfrequencies $f(\beta)$ are plotted in dependence of the wavenumber β. With regard to periodic structures, the analysis can be restricted to one unit cell while defining periodic boundary conditions on its borders and considering the irreducible Brillouin zone [9] by exploiting symmetries. Commercial software tools are available providing an eigenmode solver for the determination of the eigenvalues. Nevertheless, the process may turn out cumbersome and the results are often questionable. For this reason, the dispersion diagram is computed on two separate ways, full-wave method (Ansoft HFSS) directly applied to the periodic unit cell and Matrix-Pencil (MP) algorithm [10] as applied to the field solution of a driven problem such as the model of the prototype in Fig. 5. The MP algorithm is based on a parametric signal representation and approximates the eigenmodes by a series of complex exponentials

$$y_k = x_k + n_k = \sum_{t=1}^{M} A_t e^{\gamma_t \kappa k} + n_k \tag{2}$$

building the total field solution by superposition. The field data y_k is retrieved by sampling the field solution of the driven problem (CST MWS) with a step distance of κ along a straight line in propagation direction. The numerical noise n_k overlays the signal. The data is arranged in particular matrices (matrix pencils) formulating the eigenvalue problem. Singular value decomposition (SVD) yields the propagation constants and modes with the strongest impact are filtered out. The amplitudes are estimated according to the least mean square principle. The obtained phase constant β verifies the result from the full-wave simulation (HFSS) of the infinite periodic configuration (Fig. 8). The negative slope of the lower curve twig is only possible by LH performance due to anti-parallel group and phase velocity. Having established the balanced condition at about 4.35 GHz, the LH mode converts continuously into the RH mode for higher frequencies. To note is that the waveguide merely works in its fundamental mode without being affected by modes of the outside medium. The advantage of the MP method is that it also delivers the attenuation constant α seen in Fig. 9. For comparison, the attenuation constant was also deduced from the transmission coefficient S_{21} of the driven balanced simulation model with 40 unit cells and tapered transitions to microstrip lines by

$$\alpha\left[\mathrm{m}^{-1}\right] = -\frac{|S_{21}|[\mathrm{dB}]}{l\ 8.686[\mathrm{dB}]}, \tag{3}$$

where de-embedding was not applied and l is the total length of the simulated structure. The curve segment from 4.1 GHz to 4.7 GHz in the MP curve in Fig. 9 is drawn with a dotted line. In this frequency range, the wavelength becomes increasingly longer and the estimation of the propagation parameters via MP becomes inaccurate due to the too short observation interval. Apart from this, both curves in Fig. 9 agree very well. At 4.1 GHz the losses account to $\alpha = 1.08$ and at 4.7 GHz they produce $\alpha = 0.89$. For the very short unit cell sections with $\Delta l \approx \lambda_0 / 20$ near the balancing frequency and for the employed substrate with a loss $\tan\delta = 0.0035$ together with the Kapton foil layer with a loss $\tan\delta = 0.003$, the observed attenuation is very low and is comparable to the results found for the boxed stripline configuration in [5], which was termed "High Q".

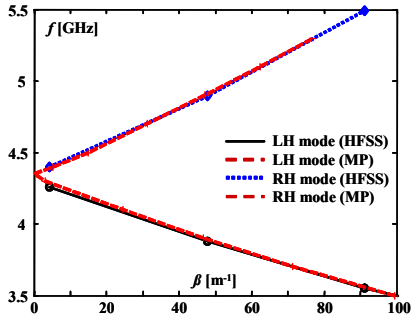

Fig. 8. Dispersion diagram verified by two separate methods, Matrix-Pencil and HFSS

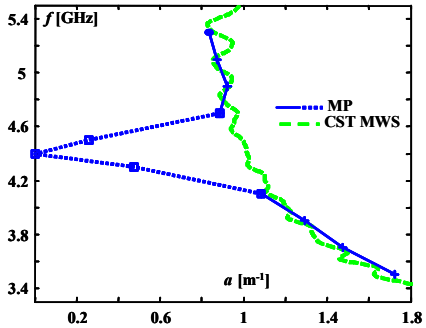

Fig. 9. Attenuation gained by simulation software and estimation technique

4. Conclusions

The proposed CRHLH waveguide meets the balanced condition at about 4.35 GHz and is matched over a broad bandwidth with reflections less than -14.56 dB. The procedure to establish the balanced state is reproducible and controllable by different means. Due to being closed, the fundamental mode is not influenced by environmental effects and stable operation is guaranteed. Therefore, merely material losses attenuate the transmitted power. The attenuation constant verified on various ways is comparable with the values reported for other "High Q" designs. The dispersion behaviour was examined and confirmed by two independent techniques. The decisive advantages of this CRHLH waveguide are its simple design, being compact and light-weight, and excellent performance despite of low-cost commercial substrate.

5. References

1. C. Caloz, T. Itoh, *Electromagnetic Metamaterials: Transmission Line Theory and Microwave Applications*, Wiley, New York, 2005.
2. A. Lai, T. Itoh, "Composite Right/Left-Handed Transmission Line Metamaterials," *IEEE Microwave Mag.*, pp. 34-50, Sep. 2004.
3. N. Marcuvitz, *Waveguide Handbook*, McGrall-Hill, New York, 1951.
4. I.A. Eshrah and A.A. Kishk, "Analysis of Left-handed Rectangular Waveguides with Dielectric-filled Corrugations Using the Asymptotic Corrugation Boundary Conditions," *IEE Proc.-Microw. Antennas Propag.,* vol. 153, no. 3, pp. 221- 225, June 2006.
5. N. Yang, C. Caloz, V. Nguyen, S. Abielmona, K. Wu, "Non-Radiative CRLH Boxed Stripline Structure with High Q Performances," *EMTS International URSI Commission B-Electromagnetic Theory Symposium*, Ottawa, Ca, July 2007.
6. D. Deslandes, K. Wu, "Analysis and Design of Current Probe Transition From Grounded Coplanar to Substrate Integrated Rectangular Waveguides," *IEEE Trans. Microwave Theory Techniq.*, vol. 53, no. 8, pp. 2487 – 494, Aug. 2005.
7. Y. Weitsch, T.F. Eibert, "A Left-Handed/Right-Handed Leaky-Wave Antenna Derived from Slotted Rectangular Hollow Waveguide," *European Microwave Conference*, Munich, Oct. 2007.
8. Y. Weitsch, T.F. Eibert, "Continuous Beam-Steering Leaky-Wave Antenna Based on Substrate Integrated Waveguide," *European Conference on Antennas and Propagation (EuCAP),* Edinburgh, 2007.
9. C. Kittel, *Introduction to Solid State Physics*, 7th ed., Wiley, New York, 1995.
10. H. Yingbo, T. K Sarkar, "Matrix Pencil Method for Estimating Parameters of Exponentially Damped/Undamped Sinusoids in Noise," *IEEE Trans. Acoustics, Speech and Signal Processing,* vol. 38, no. 5, pp. 814-824, May 1990.